Improvement in Mechanical Properties of Titanium Deformed by ECAE Process

J. Nemati[a], S. Sulaiman[b,∗], A. Khalkhali[c]

[a]Mechanical Engineering Department, Faculty of Engineering, Bu-Ali Sina University, Hamadan, Iran.

[b]Department of Mechanical and Manufacturing Engineering, University Putra Malaysia, Malaysia.

[c]School of Mechanical Engineering, Islamic Azad University, Takestan Branch, Takestan, Iran.

Article info

Abstract

In this study, annealed CP-Ti (Grade 2) was processed by Equal Channel Angular Extrusion (ECAE) up to 2 passes at a temperature of 400°C following route A with a constant ram speed of 30 mm/min through a die angle of 90° between the die channels. Mechanical properties of the extruded materials were obtained at different strain rates. The results indicated that the tensile yield stress and ultimate tensile strength of the extruded specimens increased significantly after 2 passes of ECAE process. The maximum increase for yield stress was around 90% which occurred at the pulling rate of 0.5 mm/min. The bending fatigue life of the extruded specimens improved significantly so that in low cycle fatigue regime a 700% increase in fatigue life was observed after two ECAE passes. The improvement was lower in high cycle fatigue regime. The microhardness measurement of the specimens indicated that the average microhardness of the samples increased about 140% after 2 passes. The fracture mechanism of the ECAE specimens was also studied by fractography of the fracture surface of specimens. Microstructure of the extruded specimens was also examined by optical microscopy.

1. Introduction

Titanium has excellent corrosion resistance and high strength-to-density ratio, thus the material and its alloys such as CP-Ti Grade 2 are widely used in industrial applications [1] chiefly in chemical, marine, aerospace and medical applications [2,3]. It is well-organized that grain refinement can improve the mechanical behavior of materials without changing their chemical compositions [4,5]. Severe plastic deformation (SPD) techniques have been innovated over the past few decades for producing ultrafine-grained (UFG) materials [5,6]. Equal channel angular extrusion (ECAE) is one of the SPD techniques which was developed in early 1990s by V.M. Segal in the Soviet Union [7]. In this technique, plastic deformation is caused by simple shear [7], near-nano to nanosized equiaxed grains are generated while the dispersion of orientations at high strains remains unchanged [8, 9]. In this process, a billet is extruded through a die containing two channels with equal cross-section which interconnect at an angle φ and an angle ψ which specifies the curvature of the outer point of intersection of the two channels [10,11]. Different modified ECAE techniques have been proposed to obtain improvement in homogeneity of strain in the specimens. Typical modification has been reported by Shaeri et al. [12]. Different equal channel angular pressing configurations have been investigated by Ebrahimi et al. [13] to obtain materials with the high effective strain level, more uniform strain distribution and lower pressing force. The influence of ECAE process on mechanical behaviour and microstructural evolution of many metals has extensively been studied over the past two decades. However, less attention

∗Corresponding author: S. Sulaiman (Professor)
E-mail address: shamsuddin@upm.edu.my

has been paid to titanium. Kang and Kim [14] studied the effect of T-type ECAP process on the mechanical and microstructural properties of commercially pure titanium; it was revealed that the yield and ultimate strength of CP-Ti were significantly improved and a remarkable refinement of the microstructure was obtained. There are reports implying that the ultimate tensile strength of CP-Ti (Grade 3) can reach to 1218 MPa after eight passes followed by cold rolling in liquid nitrogen [15]. Jiang et al. [16] investigated the commercial pure titanium subjected to four passes of ECAE process at a temperature of 400°C using BC route and studied the evolution of effective strain up to four passes. In the other research [17] they used 3D FEM analysis to study the temperature rise and temperature distribution in the die and CP-Ti billet during the course of deformation in ECAE process. It was shown that the temperature rise in the die and the billet was very different in different locations. Vingradove et al. [18] studied the cyclic behavior of UFG titanium processed by ECAE technique and found a remarkable improvement in fatigue limit and fatigue life of the processed material. The experimental study of using was conducted by Nagasekhar et al. [19] who examined two different processing routes to study the effect of three-pass ECAE process on the mechanical properties of CP-Ti by experiment.

The results of different studies obtained from different researchers on the effects of ECAE on different materials such as, pure copper [20,21], Fe-Mn-Si-Cr-Ni shape memory alloy [22], Al 6082 alloy [23,8], polymer materials [10], Mg-9Al-Zn alloy [11] and Al 6063 alloy [24, 25] shows that as a proposing technique, ECAE process can improve the mechanical properties of extruded materials, as well as their microstructures. All results reveal that the grains of processed materials are significantly refined even after one pass of ECAE process.

As discussed above, only several investigations have been conducted on the effect of ECAE on titanium. Moreover, a few of these investigations are purely numerical and the others are incomprehensive and have provided only a narrow information on various features of the effect of ECAE on titanium. In this study, the effect of the ECAE process on mechanical and fatigue behaviors of CP-Ti (Grade 2) was comprehensively investigated. The mechanical properties of the extruded materials were obtained at different strain rates. Fatigue resistance of the ECAEed samples was also investigated by bending fatigue test. The microstructure and grain refinement of the extruded billets was studied by optical microscopy and the fracture mechanism of the samples was examined by fractography. Microhardness of the extruded materials was also measured.
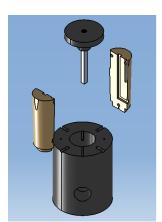
2. Material, Specimens and Testing Device

Commercially pure titanium (CP-Ti) Grade 2 was used in this work. The as-received samples were annealed at 673°K for one hour and were cooled in the furnace at a cooling rate of 293°K/hr. The chemical composition of the as-received material is given in Table 1.

Table 1
Chemical composition of CP-Ti (Wt %).

Al	V	Cr	Cu	Fe	Mn
< 0.01	< 0.05	< 0.02	< 0.02	< 0.03	< 0.02
Mo	Nb	Sn	Zr	Si	Ti
< 0.03	< 0.01	< 0.05	< 0.01	< 0.01	Base

The specimens were fabricated from $12 \times 12 \times 110$ mm billets and the ECAE tests were conducted for 1 and 2 passes using route A at a temperature of $400^0 C \pm 10°$C. The ECAE was carried out on a 60-ton Avery universal testing machine. The billets were extruded through a split die as shown in Fig. 1. The figure illustrates the schematic view of the ECAE die and the die assembly mounted on the Avery universal testing machine. As Fig. 1a suggests, the ECAE die consists of two channels intersecting at an inner angle of 90° and an outer angle of 22°. The die was equipped with the heating elements for hot extrusion.

(a)

(b)

Fig. 1. (a) A general view of the ECAE die, (b) Avery universal testing machine.

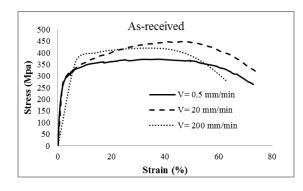**Fig. 2.** Fabrication of tensile test specimens from the extruded materials.

All ECAE process of the billets were accomplished at a constant ram speed of 30 mm/min. Before the extrusion, the billets and the die walls were lubricated with MoS_2 mineral oil to diminish the friction. The billets were first manually embedded in the die channel and were heated for 10 minutes to reach the temperature required for extrusion. The extruded billets were then used to prepare the specimens for mechanical characterization and micro-structural examination of the extruded material.

Fig. 3. Stress-strain curves of the as-received material at three different velocities.

3. Mechanical Characterization Tests

3.1. Tensile Test

Tensile test specimens were prepared from the as-received and extruded billets in the flow direction of the extrusion process according to the ASTM E8 standard as shown in Fig. 2. Tensile tests were conducted for the as-received and the extruded materials after the 1st and 2nd passes using a universal Instron testing machine.

The stress-strain curves of the extruded specimens after the first and the second passes were obtained at three pulling velocities of 0.5, 20 and 200 mm/min which correspond tentatively to the strain rates of 2.5×10^{-3}, 10^{-2} and $10^{-1}s^{-1}$. The strain rate was calculated roughly from $\dot{\epsilon} = \frac{V}{H}$ in which V and H are the pulling velocity and the gauge length of the specimens, respectively. The stress-strain curves of the as-received material at the foregoing three velocities are depicted in Fig. 3. The stress-strain curves after the first and second passes for the various velocities are illustrated in Figs. 4 and 5, respectively. The stress-strain curves for the as-received material and the extruded specimens for the velocities of 0.5, 20 and 200mm/min are illustrated in Figs. 6-8, respectively.
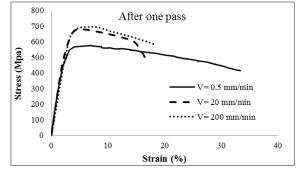

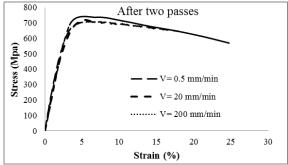**Fig. 4.** Stress-strain curves after the first pass at different velocities.

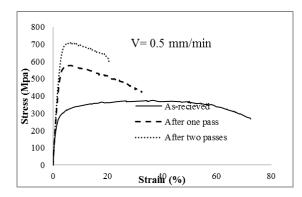**Fig. 5.** Stress-strain curves after the second pass at different velocities.

Fig. 6. Stress-strain curves of titanium for $V = 0.5$ mm/min after different passes.
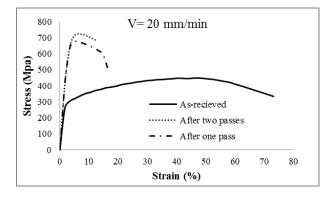

Fig. 7. Stress-strain curves of titanium for $V = 20$ mm/min after different passes.
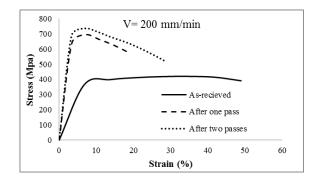

Fig. 8. Stress-strain curves of titanium for $V = 200$ mm/min after different passes.

The results shown in Fig. 6 suggest that the YS (yield stress) and UTS (ultimate tensile strength) increased from 264 to 514 MPa and 371 to 577 MPa respectively, after the 1st ECAE pass for the velocity of 0.5mm/min. The figure also indicates that the UTS increased from 371 MPa to 700 MPa after the 2nd pass and for the velocity of 0.5mm/min. This shows an impressive increase of about 88% in UTS of material. The improvements for the other velocities are still significant. As Figs. 6 and 7 show, the increase of strength of extruded materials, due to the effect of strain rate, does not show a regular trend with the increase of strain rate so that it is negligible for the

velocity of 200 mm/sec as indicated in Figs. 6-8. A comparison between the Figs. 4-6 and the Figs. 7-9 reveals that the major cause of enhancement of the strength of the processed materials is due to the extrusion rather than the strain rate.
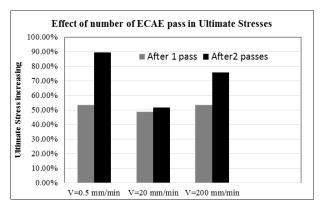

Fig. 9. The increase in ultimate strength after two passes for three different velocities.

3.2. Fatigue Test

The processed billets were subjected to bending fatigue test. Dog bone type fatigue specimens were prepared from the processed billets after the 1st and the 2nd passes. The bending fatigue tests were carried out under the stresses of 100, 110, 125, and 140 MPa on a Moore fatigue machine. Fatigue tests were also conducted on the as-received specimens. The S-N curves for different one and two passes are shown in Fig. 10. As the figure suggests, the fatigue life of the processed billets is significantly enhanced after the 1st and the 2nd passes. The fatigue failure life after one and two passes for different stresses are illustrated in Fig. 11. As the figure reveals, the processed specimens show nearly similar enhancement in fatigue life after the first and the second passes. Fig. 11 also reveals that the improvement in fatigue life of the processed materials for high-cycle fatigue (HCF) regime (100 MPa) is considerably higher than that for the low-cycle fatigue (LCF) regime (140 MPa). However, the increase percentage in fatigue life of the extruded specimens for different passes and different stresses shown in Fig. 12 suggests that the fatigue life improvement is higher for LCF regime. As it is seen in Fig. 12, the fatigue life increase for the stress of 100 MPa (HCF) is about 100% while, the increase for the stress of 140 MPa (LCF), dramatically rises to about 200% and 700% after the first and the second passes, respectively. The maximum total increase in fatigue life is approximately 700%, and occurs for the stress of 140 MPa after the second pass. However, it is presumed that the main reason for such increases might be due to crack closure that occurs in each cycle during the course of bending fatigue test of round specimens. Obviously, dur-

ing each cycle in bending fatigue test of a round bar, each point on the specimen surface experiences alternate tension and compression. The tension tends to open the crack and compression tends to close it. The alternate crack opening and closure retard the crack propagation and postpone the failure of the specimen. Evidently, the crack closure can be more effective for higher bending stresses. This may explain the cause of drastic improvement in fatigue life of low cycle fatigue tests.
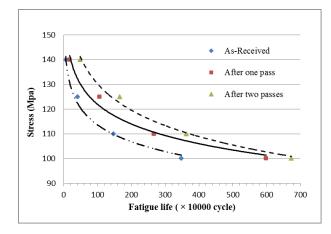

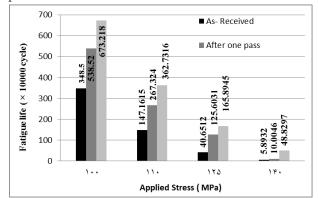**Fig. 10.** S-N curves for unprocessed and extruded specimens.

Fig. 11. The cycles to failure for different number of passes at different stresses.
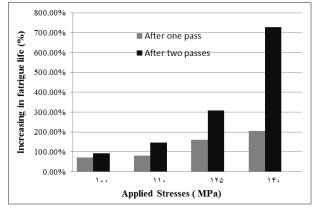

Fig. 12. The total increase in fatigue life for different applied stresses after one and two ECAE passes.

3.3. Hardness Measurement

Vickers micro hardness was measured according to the standard ASTM E-384 using a load of 500g for 30 seconds. The processed billets were cut from the middle of the extruded material along the direction of the extrusion process. Hardness was measured at thirty locations arranged in three rows (top, middle and bottom). The motivation for selecting three rows was due to non-uniformity of deformation as the top and the rear surfaces of the billets billets subjected to compression and tension during the ECAE process, respectively and the mid-surface experiences less deformation. Therefore, the mean of microhardness in each row (10 points) may provide a more realistic value for the hardness of the extruded specimens. The average Vickers Microhardness for different passes on the top, middle, and rear surfaces of the billets is illustrated in Fig. 13. As the figure suggests, the hardness of the top surface where the billet undergoes compression is slightly higher than that of the mid-surface. For the bottom surface, the situation is vice versa. The results indicated that the major improvement in the microhardness occurred after the 1st pass. In the second pass, the microhardness kept going high, but at a lower rate.
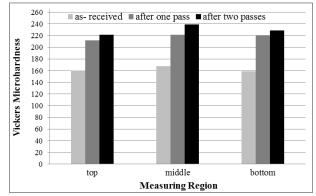

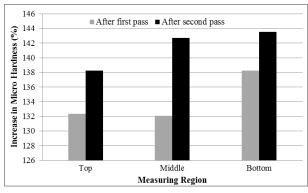**Fig. 13.** The average Vickers Microhardness for different passes on top, bottom and mid-surface of the billets.

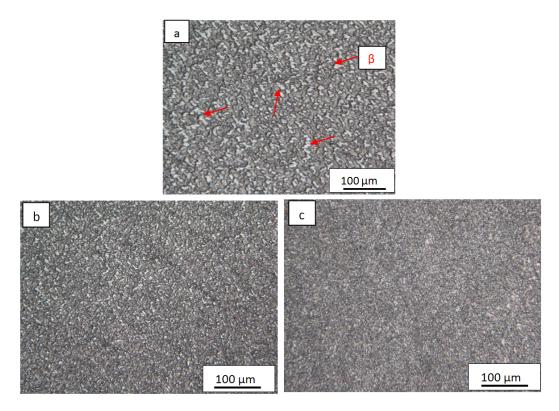**Fig. 14.** Total improvement in hardness of extruded specimens.

Fig. 15. Optical micrograph of CP-Ti (a) as-received, (b) after one pass and (c) after two passes.

The total improvement in the microhardness of the extruded specimens in the three rows after one and two ECAE passes is illustrated in Fig. 14. The figure indicates that a total of around 140% increase in hardness can be observed after 2 passes.

3.4. Metallography

Metallography of the as-received and the extruded billets after the 1th and 2nd passes was performed by optical microscopy. Specimens were cut from the as-received and the extruded titanium material Ti-CP (Grade 2) and mounted in a Bakelite. The mounted samples were then mechanically polished. The polished samples were subsequently etched using a reagent that was a solution mixture of 5-ml of nitric acid (HNO_3), 10 ml of hydrofluoric acid (HF) and 85 ml of water (H_2O). The polished and the etched surfaces of the specimens of Ti-CP (Grade 2) were studied by optical microscopy. Typical micrographs of the samples are depicted in Fig. 15. The distribution of the alpha (α) and beta (β) phases and grains can be obviously seen in the Fig. 15a. The figure Fig. 15 reveals that the primary (α) grains are intermingled with small pockets of the β grains. The white spots indicate β phase, which are distributed in the texture of α phase. The figure also indicates that the grain size remarkably decreased after two ECAE passes.

3.5. Fractography

The Fracture mechanism of all extruded specimens after tensile and fatigue tests were studied on a JEOL scanning electron microscope (SEM). Therefore, the effect of strain rate on fracture mechanism of extruded specimens was studied by fractography of the tensile tested specimens and the effect of cyclic loading on fracture mechanism was investigated by fractography of fatigue tested samples. The results are explained in the next two subsections.

3.5.1. Tensile Tested Specimens

Typical SEM pictures for 0.5 and 200 mm/min velocities are depicted in Fig. 16. In the figure Pi, denotes the ith pass. Figs. 16a-18b illustrate the fracture surfaces of the as-received specimens at three different strain rates. The dimples and the conical equiaxial microvoids seen in the fractographs indicate that fracture is ductile. The figures exhibit an irregular fracture surface related to the (hcp) phase. The fractographs of the processed samples after one and two ECAE passes are presented in Figs. 16c-16f. As it is observed, strain rate has no significant influence on the fracture mechanism, therefore the high increase in YS and UTS shown in Figs. 6-8 can be thought to be caused by strain hardening due to high dislocation pileups and grain refinement resulted from ECAE.
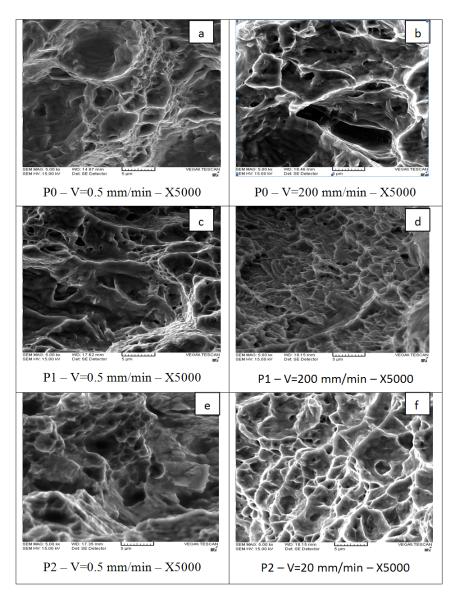
Fig. 16. SEM micrograph of extruded specimens after different ECAE passes for the velocities of 0.5 and 200 mm/min.

3.5.2. Fatigue Tested Specimens

Fracture surfaces of the fatigue samples were examined on a JEOL scanning electron microscope (SEM). Typical fractographs of the fatigue fracture surfaces of the CP-Ti (Grade 2), at different stress levels are illustrated in Fig. 17. Figs. 17b and 17e exhibit areas of populated dimples along with voids of different shapes and sizes, representing that fracture mechanism is ductile. In Figs. 17a and 17d flat regions populated with randomly distributed fine microscopic cracks are observed. In these pictures, regions of stable crack growth containing pockets of shallow striations can be observed which sign of localized micro-plastic de-

formation are. The morphology of the fractographs illustrated in Figs. 17f and 17c show the pockets of striations in the region of stable crack growth. This also represents a ductile failure. Therefore, it can be concluded that extrusion and strain rate doesn't alter the fracture mechanism of the extruded titanium.
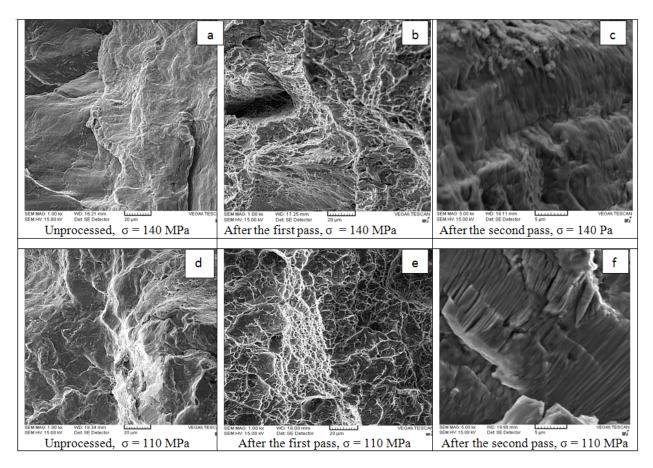
Fig. 17. Micrographs of the fracture surfaces of unprocessed and extruded specimens after the first and the second passes at the stresses of 110 and 140 MPa.

4. Conclusions

The following conclusions can be derived in this study:

1. The yield stress and the ultimate strength of the extruded specimens significantly increased after two passes of the ECAE process. The average increase was found to be around 80%, regardless of the tension velocities. The major improvement was achieved after the first pass.

2. The effect of strain rate on the strength of extruded material did not show a regular trend.

3. The elongation and hence the ductility of the extruded specimens decreased by increasing the pass number.

4. For low stresses (or HCF regime), a total increase of approximately 100% in fatigue life of the extruded material was observed after two passes. This maximum increase was 700% and was obtained for the highest applied stress (or LCF regime).

5. The improvement in fatigue life after the 1st and the 2nd passes were more or less the same.

6. The microhardness of the work pieces increased significantly during the deformation. A total of around 140% increase in hardness was observed after 2 passes.

7. Optical microscopic examinations revealed that the grain size reduced significantly after two passes.

8. Micrographs of the fracture surfaces of the tensile tested samples showing the morphology and distribution of dimples and fine microscopic voids feature reminiscent of locally ductile failure mechanisms. The fracture surfaces also exhibited an irregular fracture surface related to the (hcp) phase.

9. For the fatigue tested samples, the fracture surface morphology shows the pockets of well-defined striations in the region of stable crack growth. In the region of overload, observation revealed a healthy population of dimples intermingled with voids of varying size and shape featuring reminiscent of locally ductile failure mechanisms.

References

[1] ASME I. Properties and Selection: Nonferrous Alloys and Special-Purpose Materials, ASME Handbook, 2 (1990) 592-593.

[2] R. Chaudhari, R. Bauri, Microstructure and Mechanical Properties of Titanium Processed by Spark Plasma Sintering (SPS), Metallurgic Microstructure anu. 3 (2014) 30-35.

[3] G. Purcek, O. Saray, O. Kul, I. Karaman, G.G. Yapici, M. Haouaoui, H.J. Maier, Mechanical and wear properties of ultrane-grained pure Ti produced by multi-pass equal-channel angular extrusion, Mater. Sci. Eng. A. 517 (2009) 97-104.

[4] V.P. Basavaraj, U. Chakkingal, T.S.P. Kumar, Study of channel, angle inuence on material ow and strain inhomogeneity in equal channel angular pressing using 3D nite element simulation, J. Mater. Process. Tech. 209 (2009) 89-95.

[5] I. Kim, J. Kim, D.H. Shin, C.S. Lee, S.K. Hwang, Effects of equal channel angular pressing temperature on deformation structures of pure Ti, Mater. Sci. Eng. 342 (2003) 302-310.

[6] Y.W. Tham, M.W. Fu, H.H. Hng, M.S. Yong, Lim KB, Study of deformation homogeneity in the multi-pass equal channel angular extrusion process, J. Mater. Process. Tech. 192 (2007) 121-127.

[7] V.M. Segal, Materials processing by simple shear. Mater. Sci. Eng. 197 (1995) 157-164.

[8] E. Cerri, P.P. De Marco, P. Leo, FEM and metallurgical analysis of modied 6082 aluminium alloys processed by multi pass ECAP: Inuence of material properties and different process settings on induced plastic strain, J. Mater. Process. Tech. 209 (2009) 1550-1564.

[9] R. Luri, C.J. Luis Prez, D. Salcedo, I. Puertas, J. Len, I. Prez, J.P. Fuertes, Evolution of damage in AA-5083 processed by equal channel angular extrusion using different die geometries, Mater. Des. 211 (2011) 48-56.

[10] Q. Jianhui, M. Takuya, W. Xueli, K. Masayoshi, Plastic deformation mechanism of crystalline polymer materials in the equal channel angular extrusion process, J. Mater. Process. Tech. 212 (2012) 1528-1536.

[11] J. Jiang, Y. Wang, Z. Du, J. Qu, Y. Sun, L. Shoujing, Enhancing room temperature mechanical properties of Mg-9Al-Zn alloy by multi-pass equal channel angular extrusion, J. Mater. Process. Tech. 210 (2010) 751-758.

[12] M.H. Shaeri, F. Djavanroodi, M. Sedighi, S. Ahmadi, M.T. Salehi, SH. Seyyedein, Effect of copper tube casing on strain distribution and mechanical properties of Al-7075 alloy processed by equal channel angular pressing, J. Strain. Anal. Eng. Des. 48 (2013) 512-521.

[13] M. Ebrahimi, B. Rajabifar, F. Djavanroodi, New approaches to optimize strain behavior of Al6082 during equal channel angular pressing, J. Strain. Anal. Eng. Des. 48 (2013) 395-404.

[14] D.H. Kang, T.W. Kim, Mechanical behavior and microstructural evolution of commercially pure titanium in enhanced multi-pass equal channel angular pressing and cold extrusion, Mater. Des. 31 (2010) S54-S60.

[15] F. Zhiguo, J. Hong, S. Xiaogang, S. Jie, Z. Xiaoning, C. Xie, Microstructures and mechanical deformation behaviors of ultrane-grained commercial pure (Grade 3) Ti processed by two-step severe plastic deformation, Mater. Sci. Eng. 527 (2009) 45-51.

[16] J. Hong, F. Zhiguo, C. Xie, 3D Finite element simulation of deformation behavior of CP-Ti and working load during multi-pass equal channel angular extrusion, Mater. Sci. Eng. 485 (2008) 409-414.

[17] J. Hong, F. Zhiguo, C. Xie, Finite element analysis of temperature rise in CP-Ti during equal channel angular extrusion, Mater. Sci. Eng. 513 (2009) 109-114.

[18] A.Yu. Vinogradov, V.V. Stolyarov, S. Hashimoto, R.Z. Valiev, Cyclic behavior of ultrane-grain titanium produced by severe plastic deformation, Mater. Sci. Eng. 318 (2001) 163-173.

[19] A.V. Nagasekhar, U. Chakkingal, P. Venugopal, Candidature of equal channel angular pressing for processing of tubular commercial purity-titanium, J. Mater. Process. Tech. 173(1) (2006) 53-60.

[20] J. Nemati, G.H. Majzoobi, S. Sulaiman, B.T.H.T. Baharudin, M.A.A. Hanim, Finite element and metallurgical study of properties of deformed pure copper by ECAE at various strain rates, J. Mech. Eng. Sci. 228(9) (2014) 1461-1473.

[21] J. Nemati, G.H. Majzoobi, S. Sulaiman, B.T.H.T. Baharudin, M.A. Azmah Hanim, Improvements in the microstructure and fatigue behavior of pure copper using equal channel angular extrusion, Int. J. Miner. Metall. Mater. 21(6) (2014) 569-576.

[22] W. Zhang, L. Jiang, N. Li, W. Yuhua, Improvement of shape memory effect in an Fe-Mn-Si-Cr-Ni alloy fabricated by equal channel angular pressing, J. Mater. Process. Tech. 208 (2008) 130-134.

[23] A.S.M. Agena, A study of ow characteristics of nanostructured Al-6082 alloy produced by ECAP under upsetting test, J. Mater. Process. Tech. 209 (2009) 856-863.

[24] J. Nemati, G.H. Majzoobi, S. Sulaiman, B.T.H.T. Baharudin, M.A. Azmah Hanim, Improvements in the microstructure and fatigue behavior of pure copper using equal channel angular extrusion, Int. J. Miner. Metall. Mater. 22(4) (2015) 395-404.

[25] S. Sulaiman, J. Nemati, M. Hani Mizhir, B.T.H.T. Baharudin, G.H. Majzoobi, M.A.A. Hanim, Experimental Study of IMPact Strength of Al-6063 Alloy Processed by Equal Channel Angular Extrusion, Adv. Mater. Res. 911 (2014) 158-162.